

An Artificial Molecular Transporter

Christian Schäfer, Giulio Ragazzon, Benoit Colasson, Marcello La Rosa, Serena Silvi, and Alberto Credi^{*[a]}

The transport of substrates is one of the main tasks of biomolecular machines in living organisms. We report a synthetic small-molecule system designed to catch, displace, and release molecular cargo in solution under external control. The system consists of a bistable rotaxane that behaves as an acid–base controlled molecular shuttle, whose ring component bears a tether ending with a nitrile group. The latter can be coordinated to a ruthenium complex that acts as the load, and dissociated upon irradiation with visible light. The cargo loading/unloading and ring transfer/return processes are reversible and can be controlled independently. The robust coordination bond ensures that the cargo remains attached to the device while the transport takes place.

A key biological function of molecular machines is the controlled and directed transport of substrates within cells.^[1] While small molecules and ions diffuse to where they are needed, entities such as vesicles or organelles are too large to diffuse through the cytosol and need to be transported by motor proteins. These devices contain a motor domain that moves directionally along a track by consuming adenosine triphosphate (ATP) as a fuel, and an extremity to which appropriate cargos can be attached and detached on demand. Indeed, the development of synthetic nanoscale machines^[2] that can actively transport molecular or ionic substrates^[3] along specific directions^[4] is a stimulating task in nanoscience and can open up unconventional routes in catalysis, smart materials, energy conversion and storage, and medical therapy.^[5]

Here we present a study aimed at developing a fully synthetic^[6] small-molecule system that possesses the structural and functional elements to carry out controlled and directed transport of a nanometer-scale cargo. Our strategy (Figure 1) relies on a bistable molecular shuttle^[7]—a rotaxane in which the ring component can be displaced reversibly between two positions along the track component in response to external stimulation—whose ring component is equipped with a dock-

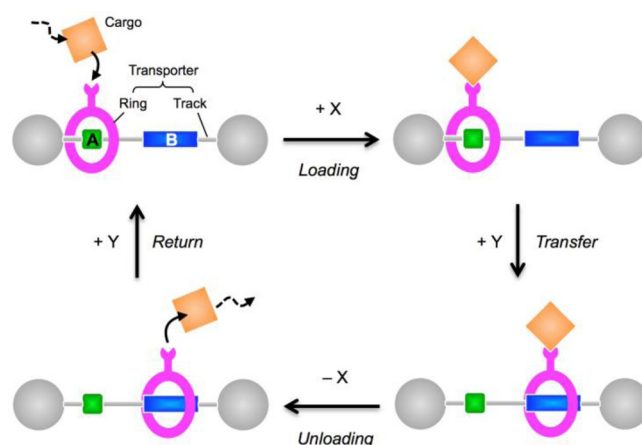


Figure 1. Design of a molecular transporter based on a bistable rotaxane shuttle and operated by two independent external stimuli, X and Y.

ing site to which the cargo can be attached and detached.^[8] From a functional point of view, the design of such a device must consider the following requirements: i) the cargo loading/unloading and ring transfer/return processes should be independent from one another, and controlled by orthogonal stimuli, ii) they should be reversible, and iii) the cargo should remain bound to the machine during the shuttling. Examples of reversible switching among more than two structurally different (supra)molecular states in response to distinct noninterfering stimuli, as shown in Figure 1 [points (i) and (ii)], are rare.^[9] Point (iii) is also very challenging, especially in combination with the first two requirements, as it calls for the use of kinetically inert bonds for the cargo-transporter link rather than dynamic supramolecular interactions.^[10]

The system is based on a [2]rotaxane architecture comprising a dibenzo[24]crown-8 (DB24C8)-type ring interlocked with a dumbbell component that possesses two different recognition sites, namely a dibenzylammonium (A) and a 4,4'-bipyridinium (B) sites (Figure 2a).^[11] Rotaxanes of this kind behave as chemically controlled bistable molecular shuttles.^[11] We prepared rotaxane 1H^{3+} in which the DB24C8 ring is endowed with a short tether ending with a nitrile unit that can serve as an anchor for the cargo (Figure 2a and Scheme 1), following published procedures (see the Supporting Information). Our results show that in acetone, the molecular ring in 1H^{3+} occupies the A site; the addition of 1 equiv of a phosphazene base ($\text{P}_1\text{-tBu}$) affords quantitatively 1^{2+} in which the ring encircles the B site. The addition of a stoichiometric amount of acid ($\text{CF}_3\text{SO}_3\text{H}$) to 1^{2+} , with respect to the previously added base, regenerates 1H^{3+} and the ring returns to the A site. In addition to ^1H NMR and UV/Vis spectroscopy, the mechanical switching

[a] Dr. C. Schäfer, G. Ragazzon, Dr. B. Colasson, M. La Rosa, Dr. S. Silvi, Prof. Dr. A. Credi
Photochemical Nanosciences Laboratory
Dipartimento di Chimica "G. Ciamician", Alma Mater Studiorum-Università di Bologna, via Selmi 2, 40126 Bologna (Italy)
E-mail: alberto.credi@unibo.it

Supporting information for this article is available on the WWW under <http://dx.doi.org/10.1002/open.201500217>.

© 2015 The Authors. Published by Wiley-VCH Verlag GmbH & Co. KGaA. This is an open access article under the terms of the Creative Commons Attribution-NonCommercial-NoDerivs License, which permits use and distribution in any medium, provided the original work is properly cited, the use is non-commercial and no modifications or adaptations are made.

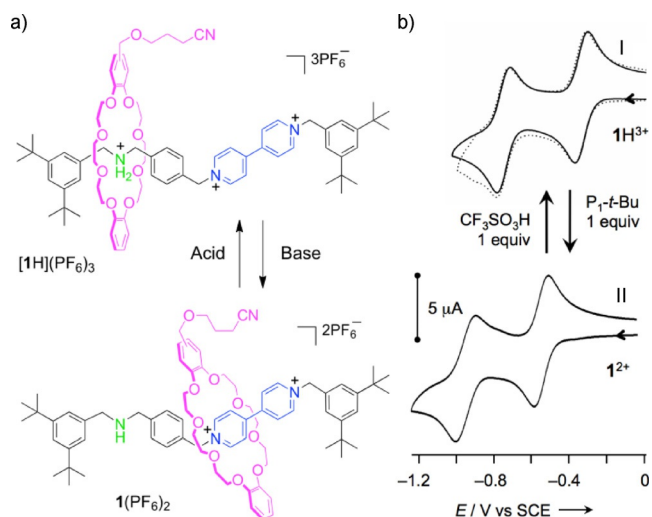
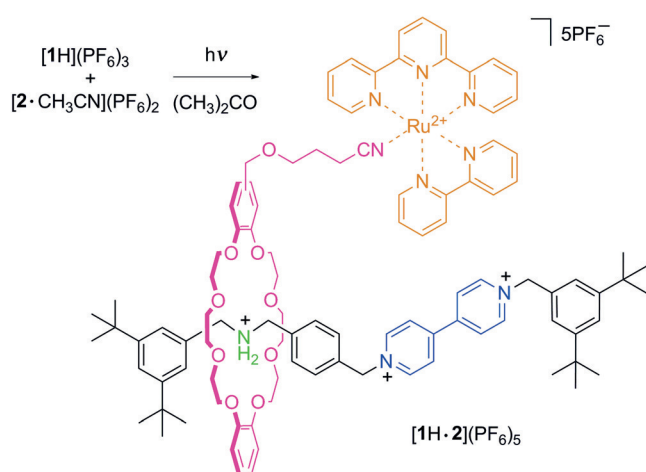


Figure 2. a) Acid–base-controlled ring shuttling in the bistable rotaxane $1H^3+/1^{2+}$. b) Cyclic voltammogram (acetone/TBAP, $400 \mu M$, $300 mVs^{-1}$) of $1H^3+$ (I, full line) and of its deprotonated form 1^{2+} (II), obtained upon addition of one equivalent of P_1-tBu . The successive addition of triflic acid in stoichiometric amount regenerates $1H^3+$ (I, dashed line).



Scheme 1. Synthesis of the cargo-loaded transporter $[1H \cdot 2]^5+$.

process schematized in Figure 2a can be conveniently observed by voltammetry. The cyclic voltammogram of $1H^3+$ (Figure 2b, trace I) exhibits two reversible monoelectronic reduction processes with $E_{1/2}$ values at -0.35 and -0.75 V versus the saturated calomel electrode (SCE), clearly assigned to the bipyridinium unit. These values are consistent with a co-conformation in which the ring is located on the A site and does not interact with the B site. The addition of base to $1H^3+$ affords 1^{2+} , whose reduction processes (Figure 2b, trace II) are both significantly shifted to more negative potentials. Such an observation clearly indicates that the bipyridinium site is now surrounded by the ring and is involved in charge-transfer interactions.^[11,12] The initial voltammetric pattern is restored upon successive addition of acid that regenerates $1H^3+$ (Figure 2b).

For the cargo loading/unloading reaction, we exploited the photochemical decooordination and thermal recoordination of ligands in appropriately designed ruthenium(II) diimine complexes (Figure 3a).^[13,14] In complexes with some distortion from the octahedral geometry, such as $[Ru(tpy)(bpy)L]^{2+}$ -type species ($tpy = 2,2',6',2''$ -terpyridine, $bpy = 2,2'$ -bipyridine), the

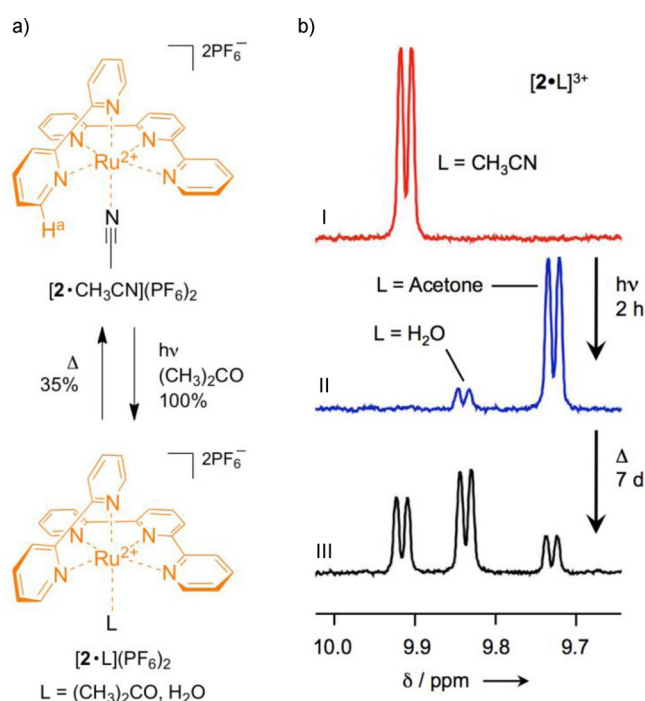


Figure 3. a) Photoinduced decooordination and thermal recoordination of a monodentate ligand in the Ru^{II} complex $[2L]^{2+}$. b) Partial 1H NMR spectra ($[D_6]acetone$, 400 MHz) of $[2 \cdot CH_3CN]^{2+}$ (I), after irradiation at $\lambda > 400$ nm for 2 h (II). Trace (III) was recorded on the irradiated solution (II) after 7 days in the dark at rt.

metal-centered (d–d) excited state (3MC) is lowered in energy such that it can be thermally populated from the lowest metal-to-ligand charge-transfer state (3MLCT) which, in turn, is efficiently obtained by excitation with visible light. As the 3MC state is strongly dissociative, light excitation in this kind of complexes results in the selective expulsion of the monodentate ligand and its replacement by solvent molecules or other entering ligands,^[14] successively, the thermally driven recoordination of the expelled ligand may take place in the dark. In recent years, the combination of this kind of reaction with cleverly designed molecular and supramolecular species has led to the construction of interesting photoactive systems.^[15]

The photochemical ligand expulsion and thermal recoordination was first investigated on the model complex^[14] $[2 \cdot CH_3CN]^{2+}$ by monitoring the resonance of the bpy proton in the α -position and close to the monodentate ligand (H^a in Figure 3a). Such a signal is observed as a doublet centered at 9.92 ppm in the 1H NMR spectrum of $[2 \cdot CH_3CN]^{2+}$ (Figure 3b, trace I). After 2 h of visible light irradiation this doublet disappears and another signal, assigned to $[2 \cdot (CH_3)_2CO]^{2+}$, shows up at 9.73 ppm, indicating that the acetonitrile ligand has been

quantitatively dissociated (Figure 3 b, trace II). Another less intense doublet at 9.84 ppm is observed, tentatively attributed to the $[2\cdot\text{H}_2\text{O}]^{2+}$ species, in which the coordination position left vacant by the leaving CH_3CN ligand is occupied by an adventitious water molecule. If the irradiated solution is left in the dark, the signal corresponding to $[2\cdot(\text{CH}_3)_2\text{CO}]^{2+}$ decreases and those related to $[2\text{L}]^{2+}$ ($\text{L}=\text{CH}_3\text{CN}$ and $\text{L}=\text{H}_2\text{O}$) are both enhanced (Figure 3 b, trace III). The integration of the NMR signals shows that after seven days, when the equilibrium is reached, the initial $[2\cdot\text{CH}_3\text{CN}]^{2+}$ complex is regenerated with 35% yield. The changes in the coordination sphere of the cargo 2^{2+} can also be followed by voltammetric methods (see the Supporting Information). The complex $[2\cdot\text{CH}_3\text{CN}]^{2+}$ shows a metal-centered reversible oxidation process at +1.35 V vs. SCE. This signal disappears upon irradiation with visible light and another irreversible process with a peak potential of $\sim +1.07$ V is observed. In agreement with the NMR results, we assign this new peak to the $\text{Ru}^{\text{II}}\text{-Ru}^{\text{III}}$ oxidation in the $[2\cdot(\text{CH}_3)_2\text{CO}]^{2+}$ species. The peak broadens and shifts further to less positive potentials upon aging in the dark. Presumably, under the conditions employed for the voltammetric experiments, the weakly bound acetone molecules are replaced by more effective ligands, such as water molecules, anions, or other impurities.

It is worth noting that $[2\cdot\text{CH}_3\text{CN}]^{2+}$ is insensitive to the addition of the base used to operate the molecular shuttle, and its photoproduct is insensitive to the presence of triflic acid. Both 1H^{3+} and 1^{2+} are not affected by visible light irradiation. Considering that the coordination bond linking the cargo to the transporter is kinetically inert at room temperature in the dark, we anticipated that our system could fulfill the functional requirements discussed above.

The cargo-loaded transporter $[1\text{H}\cdot 2]^{5+}$ was obtained by visible light irradiation of an acetone solution of $[2\cdot\text{CH}_3\text{CN}]^{2+}$ in the presence of 7 equivalents of 1H^{3+} for 10 h at room temperature (Scheme 1). As discussed above, voltammetric techniques are particularly useful to monitor the in situ operation of the molecular transporter: the two reversible monoelectronic reduction processes of the bipyridinium unit of the rotaxane are diagnostic for the position of the DB24C8-type ring along the axle (Figure 3 a), whereas the position of the $\text{Ru}^{\text{II}}\text{-Ru}^{\text{III}}$ oxidation peak can be used to determine whether the cargo is attached to the rotaxane or not.

Figure 4 shows a comparison of the differential pulse voltammetric (DPV) peaks measured in the potential window comprised between -0.7 and $+1.5$ V vs. SCE for the transporter-cargo system during its stimuli-controlled switching cycle. The DPV trace of the loaded transporter $[1\text{H}\cdot 2]^{5+}$ exhibits the expected bipyridinium reduction and the Ru-centered oxidation (Figure 4, trace I); the corresponding potential values are consistent with the ring being located on the A site and the cargo being coordinated to the nitrile moiety of the transporter. The addition of the base causes a negative shift of the reduction process and no significant change in the oxidation peak potential, indicating the displacement of the ring from A to B with the Ru complex attached to it (Figure 4, trace II). Successive irradiation in the visible ($\lambda > 400$ nm) causes the com-

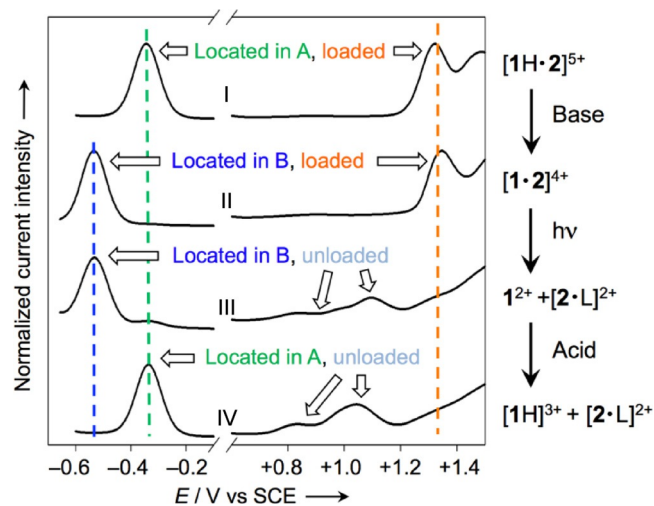


Figure 4. Differential pulse voltammograms (acetone/TBAPF₆, 400 μM , 20 mVs^{-1}) of a solution of the loaded transporter $[1\text{H}\cdot 2]^{5+}$ (I) subjected to the following sequence of stimuli: addition of 1 equiv of the $\text{P}_1\text{-tBu}$ base (II), irradiation at $\lambda > 400$ nm for 1 h (III), and addition of 1 equiv of $\text{CF}_3\text{SO}_3\text{H}$ (IV).

plete detachment of the cargo, as witnessed by the disappearance of the oxidation peak at +1.34 V and the growth of signals at less positive potentials (Figure 4, trace III). The invariance of the reduction peak at -0.53 V indicates that the ring is still occupying the B site. The DPV scan obtained after acidification of the solution (Figure 4, trace IV) shows that the unloaded ring goes back to the A site. At this point, in principle, the transporter would be ready to be reloaded with another cargo molecule. Practically, however, the thermally driven reloading in situ after the electrochemical experiments described in Figure 4 was not obtained, most likely because the weakly bound solvent molecule that occupies the coordination position made free in $[\text{Ru}(\text{tpy})(\text{bpy})]^{2+}$ after photodissociation is replaced by a stronger ligand and the complex is no longer available for recoordination to the molecular transporter (see above), which by the way is present in stoichiometric amount.

To investigate further the coupled operation of the switching processes in our system, we generated the unloaded transporter 1H^{3+} and the $[2\text{L}]^{2+}$ cargo in a 1:1 ratio by visible light irradiation of $[1\text{H}\cdot 2]^{5+}$, and we successively left the solution in the dark at room temperature (see the Supporting Information). The analysis of the DPV peak intensity indicates that the thermally driven recoordination of the Ru complex to obtain the $[1\text{H}\cdot 2]^{5+}$ species takes place with a yield of about 30%, in agreement with the results obtained for the $[2\text{L}]^{2+}$ complex. Thereafter, electrochemical measurements revealed that the so-produced reloaded transporter can be displaced by addition of base and unloaded photochemically. In this experiment, however, the addition of acid to complete the cycle (Figure 1) caused a degradation of the system, presumably because the products arising from thermal recoordination of the photodissociated 2^{2+} complex undergo a decomposition reaction in the presence of acid.

In summary, we have realized a strategy for capturing, transporting, and releasing a molecular substrate with a synthetic

molecular machine in solution under control of external signals. Owing to the orthogonality of the reactions and the stimuli at the basis of the working mechanism, the loading/unloading and transfer/return processes can be controlled independently. The robust coordination bond ensures that the cargo remains attached to the transporter during the displacement. The shuttling process is fully reversible both for the loaded and unloaded transporters, and the photochemical unloading of the cargo proceeds with high yields; the thermally driven *in situ* reloading, however, is not completely efficient and generates byproducts that interfere with the operation of the machine.

An important feature of the transporter approach is that the transport direction is fixed and dictated with nanoscale precision by the orientation of the track with respect to its surroundings. To this purpose the track should be immobilized in some way (e.g., deposited on a surface, embedded in a membrane, or held still at its extremities) while maintaining its functionality. Compartmentalization of the solution by means of membranes would also help minimizing undesired interferences of the machine with its cargo. These ambitious goals, however, are well beyond the scope of the present work. The gain in directionality is balanced by the slow transport rate: on the basis of kinetic data obtained on a parent rotaxane under similar conditions,^[11b] the shuttling is expected to need hundreds of milliseconds at room temperature, while the cargo would cover the same distance (ca. 0.7 nm)^[11,12] in less than 1 ns by diffusion.^[16] Research aimed at improving the reversibility, efficiency, and general applicability of the transport strategy, increasing the transport distance,^[17] and incorporating the rotaxanes in heterogeneous structures^[18] is underway in our laboratory.

Experimental Section

Materials. All reactants and solvents for synthesis were purchased from Sigma Aldrich and used without further purification. Dry solvents were bought dry and used directly. Spectroscopic grade (Uvasol) acetone and tetrahydrofuran (THF) were purchased from Merck; ferrocene and triflic acid were purchased from Aldrich; tetrabutylammonium hexafluorophosphate (TBAPF₆) and phosphazene base *N*-*tert*-butyl-*N,N,N',N'',N''',N''''*-hexamethylphosphorimidic triamide (P₁-*t*Bu) were purchased from Fluka. All chemicals were used as received. P₁-*t*Bu and triflic acid were added in the electrochemical cell or in the cuvette from a concentrated solution (typically 4 mM): P₁-*t*Bu was dissolved in acetone, whereas triflic acid was dissolved in THF immediately prior to use to avoid solvent polymerization.

Synthesis. The unloaded rotaxane [1H](PF₆)₃, its dumbbell-shaped and ring components, and the Ru^{II} complex [2-CH₃CN](PF₆)₂ were prepared according to published procedures, with modifications. A complete description of the synthetic methodologies and the characterization data (mass spectrometry and ¹H and ¹³C NMR) are reported in the Supporting Information.

Electrochemical measurements. Cyclic voltammetric (CV) and differential pulse voltammetric (DPV) experiments were carried out at room temperature in Ar-purged acetone (Uvasol) with an Auto-

lab 30 multipurpose instrument interfaced to a PC. A glassy carbon working electrode, a Pt wire counterelectrode, and an Ag wire pseudoreference electrode were employed; ferrocene was present as an internal standard. The concentration of the compounds under examination comprised between 2×10^{-4} and 4×10^{-4} M; TBAPF₆ (0.04 M) was the supporting electrolyte. Cyclic voltammograms were obtained at sweep rates varying typically from 0.02 to 1 V s⁻¹; DPVs were performed with a scan rate of 20 mV s⁻¹, a pulse height of 75 mV, and a duration of 40 ms.

UV/Vis spectroscopy and photochemistry. Absorption spectra were recorded with a Varian Cary 50Bio, Agilent Technologies Cary 300, and PerkinElmer Lambda45 spectrophotometers, on air-equilibrated acetone solutions at rt (~20 °C), with concentrations ranging from 1.0×10^{-5} to 2.5×10^{-3} M. Solutions were examined in 1 cm or 1 mm spectrofluorimetric quartz cells. Photochemical reactions were performed on thoroughly stirred acetone solutions at rt (ca. 20 °C) using a 150 W tungsten halogen lamp equipped with a cutoff filter ($\lambda = 388$ nm). Samples were irradiated either directly in the electrochemical cell or in a sealed cuvette. Further NMR and UV/Vis spectra and voltammetric results of switching experiments carried out on both the unloaded and loaded molecular transporters are reported in the Supporting Information.

Acknowledgements

This work was supported by the Ministero dell'Istruzione, dell'Università e della Ricerca (PRIN project "InfoChem"), the University of Bologna (FARB project "SLaMM"). B. C. thanks the Université Paris Descartes, Sorbonne Paris Cité and the Centre National de la Recherche Scientifique (CNRS) for a "délégation". C. S. thanks the Institute of Advanced Studies of the University of Bologna for a research fellowship.

Keywords: molecular machines · molecular shuttles · nanoscience · photochemistry · rotaxane

- [1] a) D. S. Goodsell, *Bionanotechnology*, Wiley, Hoboken, **2004**; b) *Molecular Motors* (Ed.: M. Schliwa), Wiley-VCH, Weinheim, **2003**.
- [2] a) V. Balzani, A. Credi, M. Venturi, *Molecular Devices and Machines, 2nd Ed.*, Wiley-VCH, Weinheim, **2008**; b) E. R. Kay, D. A. Leigh, F. Zerbetto, *Angew. Chem. Int. Ed.* **2007**, *46*, 72–196; *Angew. Chem.* **2007**, *119*, 72–196; c) S. Erbas-Cakmak, D. A. Leigh, C. T. McTernan, A. L. Nussbaumer, *Chem. Rev.* **2015**, *115*, 10081–10206.
- [3] a) G. Ragazzon, M. Baroncini, S. Silvi, M. Venturi, A. Credi, *Nat. Nanotechnol.* **2014**, *10*, 70–75; b) C. Cheng, P. R. McGonigal, S. T. Schneebeli, H. Li, N. A. Vermeulen, C. Ke, J. F. Stoddart, *Nat. Nanotechnol.* **2015**, *10*, 547–553.
- [4] a) F. C. Simmel, *ChemPhysChem* **2009**, *10*, 2593–2597; b) M. von Delius, E. M. Geertsema, D. A. Leigh, *Nat. Chem.* **2010**, *2*, 96–101; c) R. A. Muscat, J. Bath, A. J. Turberfield, *Nano Lett.* **2011**, *11*, 982–987.
- [5] a) H. Gu, S.-J. Kiao, N. C. Seeman, *Nature* **2010**, *465*, 202–205; b) J. Wang, B. L. Feringa, *Science* **2011**, *331*, 1429–1432; c) B. Lewandowski, G. De Bo, J. W. Ward, M. Pappmeyer, S. Kuschel, M. J. Aldegunde, P. M. E. Gramlich, D. Heckmann, S. M. Goldup, D. D'Souza, A. E. Fernandes, D. A. Leigh, *Science* **2013**, *339*, 189–193; d) M. Xue, J. I. Zink, *J. Am. Chem. Soc.* **2013**, *135*, 17659–17662; e) S. Chao, C. Romuald, K. Fournel-Marotte, C. Clavel, F. Coutrot, *Angew. Chem. Int. Ed.* **2014**, *53*, 6914–6919; *Angew. Chem.* **2014**, *126*, 7034–7039; f) Q. Li, G. Fuks, E. Moulin, M. Maaloum, M. Rawiso, I. Kulic, J. T. Foy, N. Giuseppone, *Nat. Nanotechnol.* **2015**, *10*, 161–165; g) A. Martinez-Cuevza, S. Valero-Moya, M. Alajarin, J. Bernal, *Chem. Commun.* **2015**, *51*, 14501–14504.

- [6] For controlled transport of cargos with synthetic DNA machines, see Refs. 4c, 5a and: T.-G. Cha, J. Pan, H. Chen, J. Salgado, X. Li, C. Mao, J. H. Choi, *Nat. Nanotechnol.* **2013**, *9*, 39–43.
- [7] a) R. A. Bissell, E. Cordova, A. E. Kaifer, J. F. Stoddart, *Nature* **1994**, *369*, 133–137; b) S. Silvi, M. Venturi, A. Credi, *J. Mater. Chem.* **2009**, *19*, 2279–2294.
- [8] For rotaxanes with functional units attached to the ring component, see Ref. [5b] and: a) A. Mateo-Alonso, C. Ehli, G. M. A. Rahman, D. M. Guldi, G. Fioravanti, M. Marcaccio, F. Paolucci, M. Prato, *Angew. Chem. Int. Ed.* **2007**, *46*, 3521–3525; *Angew. Chem.* **2007**, *119*, 3591–3595; b) H. Zhang, B. Zhou, H. Li, D.-H. Qu, H. Tian, *J. Org. Chem.* **2013**, *78*, 2091–2098; c) V. Bleve, C. Schäfer, P. Franchi, S. Silvi, E. Mezzina, A. Credi, M. Lucarini, *ChemistryOpen* **2015**, *4*, 18–21.
- [9] a) R. Ballardini, V. Balzani, M. Clemente-Leon, A. Credi, M. T. Gandolfi, E. Ishow, J. Perkins, J. F. Stoddart, H.-R. Tseng, S. Wenger, *J. Am. Chem. Soc.* **2002**, *124*, 12786–12795; b) J. V. Hernandez, E. R. Kay, D. A. Leigh, *Science* **2004**, *306*, 1532–1537; c) D. Qu, Q. Wang, H. Tian, *Angew. Chem. Int. Ed.* **2005**, *44*, 5296–5299; *Angew. Chem.* **2005**, *117*, 5430–5433; d) B. Ferrer, G. Rogez, A. Credi, R. Ballardini, M. T. Gandolfi, V. Balzani, Y. Liu, H.-R. Tseng, J. F. Stoddart, *Proc. Natl. Acad. Sci. USA* **2006**, *103*, 18411–18416; e) T. Avellini, H. Li, A. Coskun, G. Barin, A. Trabolsi, A. N. Basuray, S. K. Dey, A. Credi, S. Silvi, J. F. Stoddart, M. Venturi, *Angew. Chem. Int. Ed.* **2012**, *51*, 1611–1615; *Angew. Chem.* **2012**, *124*, 1643–1647; f) H. Cheng, H. Zhang, Y. Liu, *J. Am. Chem. Soc.* **2013**, *135*, 10190–10193.
- [10] J. Li, Y. Li, Y. Guo, J. Xu, J. Lv, Y. Li, H. Liu, S. Wang, D. Zhu, *Chem. Asian J.* **2008**, *3*, 2091–2096.
- [11] a) P. R. Ashton, R. Ballardini, V. Balzani, I. Baxter, A. Credi, M. C. T. Fyfe, M. T. Gandolfi, M. Gómez-López, M.-V. Martínez-Díaz, A. Piersanti, N. Spencer, J. F. Stoddart, M. Venturi, A. J. P. White, D. J. Williams, *J. Am. Chem. Soc.* **1998**, *120*, 11932–11942; b) S. Garaudée, S. Silvi, M. Venturi, A. Credi, A. H. Flood, J. F. Stoddart, *ChemPhysChem* **2005**, *6*, 2145–2152.
- [12] J. D. Badjic, C. M. Ronconi, J. F. Stoddart, V. Balzani, S. Silvi, A. Credi, *J. Am. Chem. Soc.* **2006**, *128*, 1489–1499.
- [13] a) J. Van Houten, R. J. Watts, *Inorg. Chem.* **1978**, *17*, 3381–3385; b) A. Juris, V. Balzani, F. Barigelletti, S. Campagna, P. Belser, A. von Zelewsky, *Coord. Chem. Rev.* **1988**, *84*, 85–277.
- [14] C. R. Hecker, P. E. Fanwick, D. R. McMillin, *Inorg. Chem.* **1991**, *30*, 659–666.
- [15] a) E. R. Schofield, J.-P. Collin, N. Gruber, J.-P. Sauvage, *Chem. Commun.* **2003**, 188–189; b) P. Mobian, J.-M. Kern, J.-P. Sauvage, *Angew. Chem. Int. Ed.* **2004**, *43*, 2392–2395; *Angew. Chem.* **2004**, *116*, 2446–2449; c) S. Bonnet, J.-P. Collin, J.-P. Sauvage, *Inorg. Chem.* **2006**, *45*, 4024–4034; d) S. Bonnet, B. Limburg, J. D. Meeldijk, R. J. M. Klein Gebbink, J. A. Killian, *J. Am. Chem. Soc.* **2011**, *133*, 252–261; e) M. Frascioni, Z. Liu, J. Lei, Y. Wu, E. Strelakova, D. Malin, M. W. Ambrogio, X. Chen, Y. Y. Botros, V. L. Cryns, J.-P. Sauvage, J. F. Stoddart, *J. Am. Chem. Soc.* **2013**, *135*, 11603–11613; f) B. A. Albani, B. Pena, N. A. Leed, N. A. B. G. de Paula, C. Pavani, M. S. Baptista, K. R. Dunbar, C. Turro, *J. Am. Chem. Soc.* **2014**, *136*, 17095–17101.
- [16] The diffusion time can be estimated with the equation expressing the mean-square displacement for a three-dimensional random walk, $\langle r^2 \rangle = 6Dt$, taking $\langle r^2 \rangle = 1 \text{ nm}^2$ and $D = 1 \times 10^{-5} \text{ cm}^2 \text{ s}^{-1}$. See H. C. Berg, *Random walks in biology*, Princeton University Press, Princeton, **1993**.
- [17] P. G. Young, K. Hirose, Y. Tobe, *J. Am. Chem. Soc.* **2014**, *136*, 7899–7906.
- [18] a) V. Fasano, M. Baroncini, M. Moffa, D. Iandolo, A. Camposeo, A. Credi, D. Pisignano, *J. Am. Chem. Soc.* **2014**, *136*, 14245–14254; b) R. Zappacosta, A. Fontana, A. Credi, A. Arduini, A. Secchi, *Asian J. Org. Chem.* **2015**, *4*, 262–270.

Received: November 26, 2015

Published online on December 30, 2015